Neuron
Article

Entrainment of Neocortical Neurons and Gamma Oscillations by the Hippocampal Theta Rhythm

Anton Sirota,[1] Sean Montgomery,[1] Shigeyoshi Fujisawa,[1] Yoshikazu Isomura,[1,2] Michael Zugaro,[1,3] and György Buzsáki[1,*]
[1]Center for Molecular and Behavioral Neuroscience, Rutgers, The State University of New Jersey, 197 University Avenue, Newark, NJ 07102, USA
[2]Present address: Neural Circuit Theory, RIKEN Brain Science Institute, 2-1 Hirosawa, Wako, Saitama 351-0198, Japan
[3]Present address: CNRS - Collège de France, LPPA, UMR 7152, 11, place Marcelin Berthelot, 75005 Paris, France
*Correspondence: buzsaki@axon.rutgers.edu
DOI 10.1016/j.neuron.2008.09.014

SUMMARY

Although it has been tacitly assumed that the hippocampus exerts an influence on neocortical networks, the mechanisms of this process are not well understood. We examined whether and how hippocampal theta oscillations affect neocortical assembly patterns by recording populations of single cells and transient gamma oscillations in multiple cortical regions, including the somatosensory area and prefrontal cortex in behaving rats and mice. Laminar analysis of neocortical gamma bursts revealed multiple gamma oscillators of varying frequency and location, which were spatially confined and synchronized local groups of neurons. A significant fraction of putative pyramidal cells and interneurons as well as localized gamma oscillations in all recorded neocortical areas were phase biased by the hippocampal theta rhythm. We hypothesize that temporal coordination of neocortical gamma oscillators by hippocampal theta is a mechanism by which information contained in spatially widespread neocortical assemblies can be synchronously transferred to the associative networks of the hippocampus.

INTRODUCTION

An essential aspect of cortical operation is that the results of local computations are integrated globally. Although the mechanisms of such local-global interactions are not well understood (Buzsáki, 2006; Dehaene et al., 2003; Engel et al., 2001; Varela et al., 2001), network oscillations have been assumed to play a critical role (Destexhe and Sejnowski, 2001; Engel et al., 2001). A general feature of cortical oscillations is that slow rhythms engage large areas and effectively modulate the more localized and shorter-lived fast oscillations (Bragin et al., 1995; Chrobak and Buzsáki, 1998a; Lakatos et al., 2005). Integration of information between different structures, such as the hippocampus and neocortex, is a special case of global coordination.

In waking cortical networks, local cell assembly organization is reflected in the occurrence of gamma oscillations (Gray and Singer, 1989; Harris et al., 2003). In the hippocampus, "activation" state is reflected by highly synchronous theta frequency oscillations (Buzsáki, 2002; Grastyán et al., 1959; Green and Arduni, 1954; Jouvet, 1969; Vanderwolf, 1969), which has been hypothesized to serve as a temporal organizer for a variety of functions (Bland, 1986; O'Keefe and Burgess, 2005). Theta-modulated cells have been found in the entorhinal cortex (Alonso and Garcia-Austt, 1987; Chrobak and Buzsáki, 1998b), perirhinal cortex (Muir and Bilkey, 1998), cingulate cortex (Colom et al., 1988; Holsheimer, 1982; Leung and Borst, 1987), prefrontal cortex (Hyman et al., 2005; Jones and Wilson, 2005; Siapas et al., 2005), amygdala (Collins et al., 1999; Paré and Gaudreau, 1996), anterior thalamus (Vertes et al., 2001), mammillary bodies, the supramammillary nucleus (Kocsis and Vertes, 1994), and the subiculum (Anderson and O'Mara, 2003). In addition, the rhythmic synchronous output of the hippocampus has been suggested to time the initiation of voluntary movements (Berg et al., 2006; Buño and Velluti, 1977; Macrides et al., 1982; Semba and Komisaruk, 1978) and gate sensory information (cf. Bland, 1986). Mainly on the basis of these behavioral results, the influence of hippocampal theta oscillations on neurons outside the limbic areas has been repeatedly conjectured (Bland, 1986; Buño and Velluti, 1977; Miller, 1991; Semba and Komisaruk, 1978), but experimental evidence to support this function is lacking. Phase modulation is a potential mechanism by which the hippocampus can coordinate disparate neocortical cell assemblies. To test this hypothesis and expand on previous works (Hyman et al., 2005; Jones and Wilson, 2005; Siapas et al., 2005), we recorded unit activity and local field potentials (LFP) from multiple neocortical regions, including primary sensory areas and the medial prefrontal cortex (PFC), along with hippocampal activity in rats and mice. We report here that a significant fraction of neurons in all recorded neocortical areas and locally emerging gamma oscillations are phase modulated by the hippocampal theta rhythm.

RESULTS

To investigate the effect of hippocampal theta oscillations on neocortical networks we recorded multiple single units and LFP in the associative and primary somatosensory (Figure 1A,

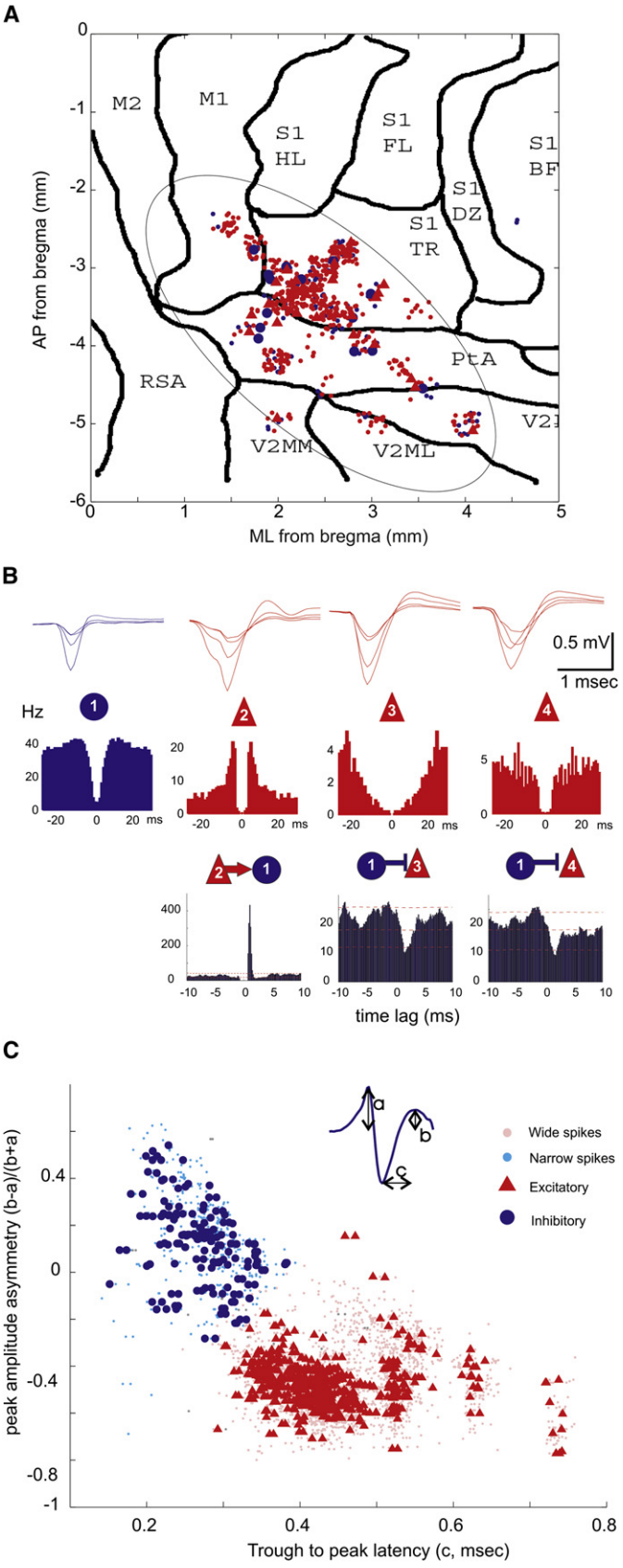

Figure 1. Separation of Putative Neocortical Interneurons and Pyramidal Cells

(A) Topographic distribution of putative pyramidal cells (red dots, triangles) and interneurons (small and larger blue dots) recorded from the parietal cortical area in all animals. Each symbol corresponds to a neuron (n = 767 from 24 rats), the position of which was inferred from implantation coordinates of the electrodes on a flattened cortical map. M1, M2, motor cortex; S1, primary somatosensory cortex; HL, hindlimb; FL, forelimb; BF, barrel field; TR, trunk; PtA, posterior associative area; V2MM, V2ML, secondary visual cortex; RSA, retrosplenial cortex.

(B) Average wide band-recorded waveforms (1 Hz-5 kHz; upper row) and autocorrelograms (middle row) of four example units. Superimposed traces were recorded by the four tetrode sites. Bottom row, short-latency monosynaptic interactions between neuron pairs, as revealed from the crosscorrelograms. Neuron 2 excites neuron 1 (recorded on the same electrode), which in turn, inhibits neurons 3 and 4 (on a different electrode). Lines indicate mean and 1% and 99% global confidence intervals.

(C) Neurons were clustered according to waveform asymmetry and mean filtered spike width (see inset; 0.8–5 kHz). Each symbol corresponds to an isolated unit (n = 2716, including neurons recorded from the medial prefrontal cortex, mPFC). Putative excitatory and inhibitory neurons form separate clusters. Circles/triangles in (A) and (C) correspond to inhibitory and excitatory neurons identified by monosynaptic interactions (as in [B]; Barthó et al., 2004).

referred to here as "parietal") areas or the anterior cingulate and prelimbic divisions of the medial prefrontal cortex (PFC) in 28 rats and 11 mice during task performance on an elevated maze and/or REM sleep. The reference theta oscillation signal was always derived from the CA1 pyramidal layer of the dorsal hippocampus (see Figure S1 available online).

Segregation of Principal Cells and Inhibitory Interneurons

Network activity in the cortex is organized by the interplay of various classes of principal cells and inhibitory interneurons (Markram, 2006; Somogyi and Klausberger, 2005). Since these two major classes of neurons have different firing rates, circuit and resonant properties and contribute differentially to cortical operations (Beierlein et al., 2000; Freund and Buzsáki, 1996; Markram, 2006), experimental identification, and separation of excitatory principal cells and inhibitory neurons are important for studying the effects of afferent signals on neocortical activity. Simultaneous recording of multiple single units in a small neocortical volume allowed us to identify putative principal cells and inhibitory interneurons (Figures 1B and 1C; Barthó et al., 2004; Constantinidis and Goldman-Rakic, 2002; Tierney et al., 2004; see Supplemental Data). The majority of the recorded neocortical units were classified as putative pyramidal cells (n = 2297, 85% in rats, n = 72, 84% mice) and the minority as putative interneurons (n = 343, 13% in rats; n = 14, 16% in mice).

Hippocampal Theta Phase-Locking of Neocortical Neurons

Several statistical methods were used to quantify the significance and magnitude of theta phase-locking of neocortical cells (Figures 2A–2D). Using Rayleigh tests (Figures 2E and 2F; α = 0.05) we found that the percentage of significantly modulated interneurons was higher than that of pyramidal cells in both parietal (32% versus 11%, respectively) and prefrontal cortices (46% versus 28%, respectively). The percentage of both cell types with significant theta phase-locking was significantly higher in PFC than in the parietal area (Figures 2E and 2F), but the fractions of significantly modulated neurons within the parietal subregions were similar (interneurons/pyramidal cells; S1: 33%/10%; posterior associative area [PtA]: 27%/11%). In contrast, the depth of theta modulation (von Mises concentration coefficient) of pyramidal cells was consistently higher than that of the interneurons (Figure S2). Additional analyses, including nonparametric tests, fit of a mixture model and spectral analysis, aimed to control for the assumptions of the Rayleigh test and gave comparable results (Supplemental Data; Figures S2 and S3). The preferred phases of significantly modulated neurons were similarly and broadly distributed for both interneurons and pyramidal cells, with highest density corresponding to the peak/descending phase of the CA1 theta cycle (Figures 2G and 2H).

Theta phase-locking of neocortical neurons occurred during both running on the track and REM sleep. Neurons could be significantly phase locked to theta in either one or both of these theta-associated states (Figures 2I–2L). In the subset of significantly modulated neurons that were recorded in both states the preferred phase of theta modulation was correlated across states (Figure 2L; $R_{circular}$ = 0.42). On average, the preferred phase of the population was significantly delayed during running compared to during REM in PFC, but not in the parietal cortex ($\sim 75^{\circ}$; circular anova, $p < 10^{-5}$ and $p > 0.3$, respectively; Figures 2K and 2L). Comparable results were obtained in mice (Figure S4). Approximately 60% of putative interneurons (of n = 14 total) and 35% of pyramidal neurons (of n = 72) were significantly (α = 0.05) modulated, with similar theta phase preferences across the population. These findings in rats and mice show that hippocampal theta oscillations impose a detectable phase-modulatory effect on the firing rate of neocortical neurons.

Locally Generated Neocortical Gamma Oscillations

Before examining the impact of theta phase on gamma oscillations, we investigated the local origin of gamma activity in the neocortex. First, we estimated the coherence between spike trains of pairs of neurons with sufficiently high firing rates (>5Hz). In a fraction of them (n = 123 pairs, 15% ± 10% of all pairs) significant coherence peaks between 30 and 140 Hz were found (Figure S5). Next, we computed the coherence between unit firing and the LFP recorded at multiple sites of the silicon probe (Figure 3A). Spikes were locked most coherently in a narrow band of a particular gamma frequency to the LFP in a localized cortical volume (Figures 3B–3D, 3F, and S6A–S6C). Spike-LFP coherence in the gamma band was in general, though not always, highest around the soma of the respective unit and decreased with distance (Figures 3D and 3E). Most neurons were phase-locked to the troughs of LFP gamma cycles (Figure 3G). In a related approach, we calculated average spectral power in short (50–100 ms) epochs temporally surrounding the action potentials of single neurons. Similar to coherence analysis, these "spike-triggered" spectra showed strong correlation between the firing of a subset of neurons and the LFP power within specific narrow ranges of gamma frequency oscillations in localized neocortical areas (Figures 3H, 3I, and S6D–S6I). Analysis of spectra at various time lags from the triggering spike showed that increases of the space-frequency localized power were transient, reaching maximum within 0–100 ms from the reference spike (Figure S6). Some data sets contained simultaneously recorded neurons that were phase-locked or correlated with gamma oscillations, which were localized at the same location (putative layer and/or column) and/or frequency (e.g., Figures 3C, 3D, 3H, and 3I), indicating that gamma oscillations with particular localization and/or frequency are associated with the activity of unique groups of neurons.

Synchronization of pools of neurons was tentatively associated with transient increases of LFP power at specific locations and narrow gamma frequency bands. Because of volume conduction and the linear summation of different transient gamma oscillations with variable amplitudes and frequencies continuous summation of spectral power in the gamma band may not yield reliable results. Therefore, we devised two alternative approaches. The first approach is based on the monotonous decay of power away from gamma sources. Exploiting our multiple site recordings, a subset of well isolated gamma bursts were detected as local maxima of the spectral power in time, space, and frequency, and the detected events tended to cluster (e.g., Figure 4). The second approach for the detection of gamma

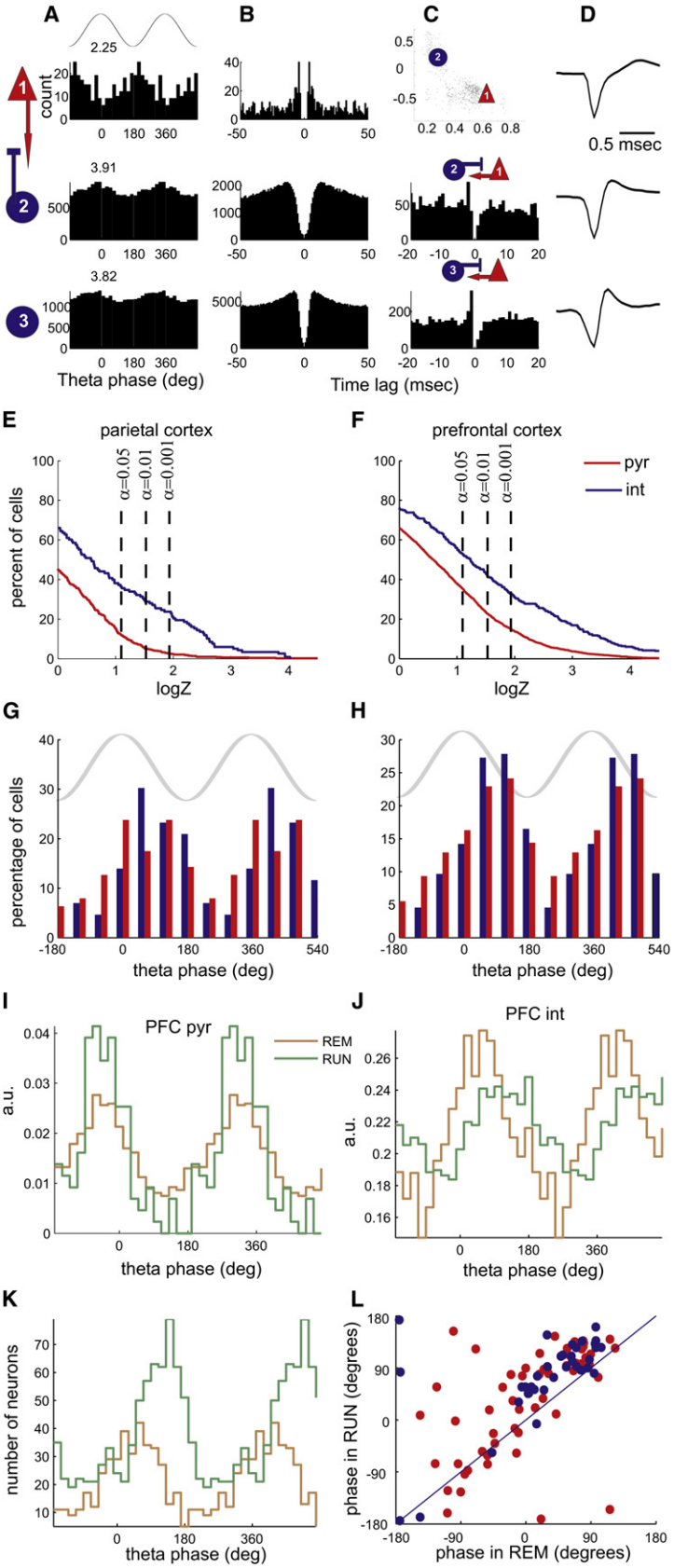

Figure 2. Hippocampal Theta Phase Modulation of Neocortical Neurons

(A–D) Each row corresponds to a single unit from the parietal-S1 area. (A) Theta phase histograms of neurons firing during REM sleep. Top, cartoon theta wave from the CA1 pyramidal layer. Numbers above, logZ statistics. Columns (B)–(D) characterize the units. (B) Autocorrelograms of the respective units. (C) Wave shape parameter scatterplot (top) and crosscorrelograms between the respective neuron and its monosynaptic partner (rows 2 and 3). (D) Average wideband-recorded (1 Hz–5 kHz) spike wave forms.

(E and F) Cumulative density function of phase modulation statistics (logZ) for putative pyramidal cells (pyr, red) and interneurons (int, blue) from the parietal (E) and mPFC (F). The plot is normalized to show the percentage of neurons (y axis) with logZ statistics greater than given value (*x* axis), y = P(X > x).

(G and H) Distribution of preferred phases for all significantly modulated ($p < 0.05$) neurons in the parietal cortex (G) and mPFC (H). Both cell types fire preferentially at around the peak/descending slope of hippocampal theta (phase 0°–90°).

(I and J), Theta phase histograms of an example pyramidal cell (I) and interneuron (J) from PFC during REM sleep and running on an elevated maze. Note that both neurons are significantly modulated in both states. Note also shift of phase preference of the interneuron.

(K) Phase histograms of preferred phases of all significantly modulated neurons during REM and awake running. Note phase shift of the population to the later theta phase during running.

(L) Scatterplot of preferred phases of neurons significantly modulated in both REM and RUN conditions (n = 98). Red, putative pyramidal cells; blue, putative inhibitory neurons.

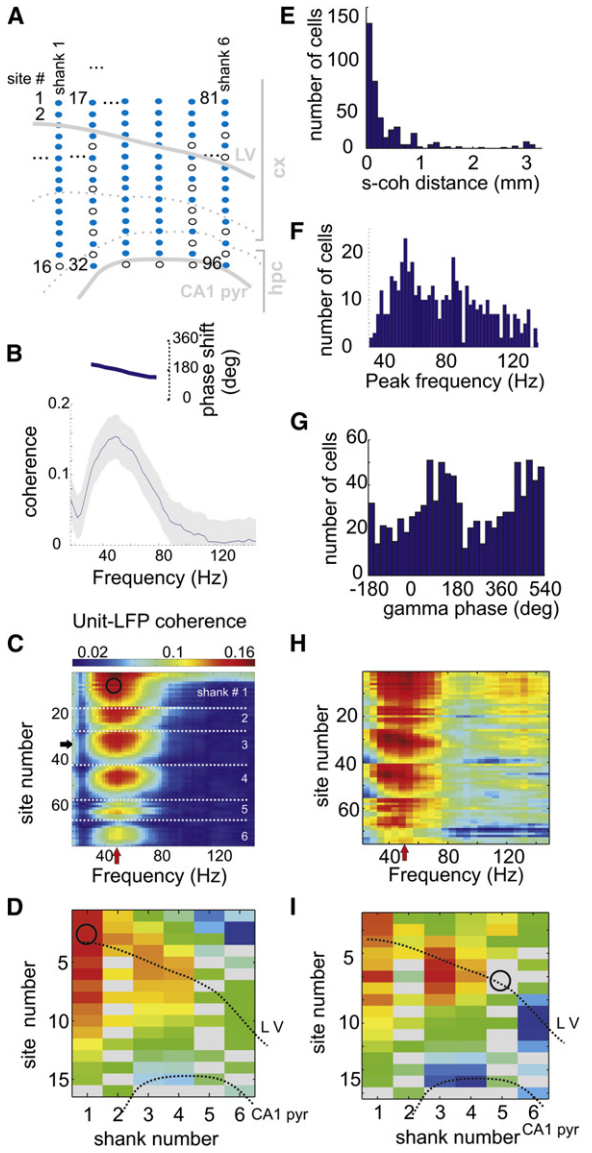

Figure 3. Gamma Frequency Band Synchronization of Neocortical Neurons

(A) Anatomical layout indicating the location of recording sites of the silicon probe used in the examples (B)–(D) and (H) and (I). Shanks are spaced by 300 μm, and each contains 16 recording sites 100 μm apart. Malfunctioning recording sites are shown as open circles and omitted from further analysis.

(B) Coherence (gray shading, 95 percentile confidence bands; inset, phase spectrum) between the spike train of a putative interneuron and the LFP at one recording site (horizontal arrow in [C]) in the parietal area.

(C) Coherence (color-coded) in the gamma range between a putative interneuron (recorded at site marked by a circle) and LFPs at all recording sites of the six shank silicon probe (y axis; 76 of 96; the remaining 20 sites with artifacts were excluded; see Supplemental Data). White dotted lines separate recording sites from adjacent shanks. Note increase of unit-LFP coherence at a preferred frequency (red vertical arrow, 40–50 Hz) and preferred depth/sites.

(D) Unfolding the unit-LFP coherence from (C) at the maximal frequency (red arrow in [C]) to a spatial map. The CA1 pyramidal layer and the approximate cortical layer 5 (dotted lines) are superimposed for spatial orientation. Circle, location of the soma of the recorded unit. Note that coherence (color) is highest locally and remains relatively high in a spatially contiguous volume up to 1 mm. Gray rectangles, sites with artifacts.

(E–G) Group statistics for all unit-LFP pairs with significant coherence (n = 456 units). (E) Distribution of the distances between the site of the recorded neuron (putative location of the soma) and the maximum unit-LFP coherence (s-coh distance). (F) Distribution of peak frequencies of unit-LFP coherence. (G) Distribution of preferred firing phases within the gamma cycle (trough, 180°).

(H and I) Example of spike triggered spectral analysis for a unit (same session as [A]–[D]). (H) Spike-triggered average power spectra (minus the power spectra calculated over the entire session; see Supplemental Data) color coded (red, relative increase of power; blue, relative decrease) for all channels (y axis). (I) Unfolding the spike-triggered power at preferred frequency from (H) to a spatial map. Circle, site of the recorded unit (putative soma location) used for triggering. Note that the power reaches maximum at a narrow "preferred" frequency band and at neighboring recording sites.

bursts is based on the covariance of spectral power in space (between different recording sites) and frequency (between different frequency bins, see Supplemental Data). Briefly, we performed factor analysis (principal component analysis followed by the Varimax rotation of the eigenvectors) of the spectral power in the gamma frequency range (30–150 Hz) seeking basis vectors that most parsimoniously captured the structure of power covariation between different frequency bins at different recording sites (Figures 3H, 3I, and 4D). The end product of this analysis was a set of factors, each of which was characterized by a vector of factor loadings reflecting the contribution of the respective frequency bins and recording sites to spectral power covariations. Projection of the spectra on these factors yielded a time series, termed factor scores, which reflect the strength of a given factor at any moment in time (Figure S7). Each of these factors could correspond to gamma oscillations with a distinct frequency and location pattern, and thus we refer to them as gamma frequency location (gFL) factors, or gFLs.

Several (from 0 to 32) gFLs were selected in each session based on explained covariance (Figure 5A). The space-frequency profiles of gFL factor loadings shared many features with those produced by unit-LFP spectral analysis and local maxima analysis. First, the gFL profiles showed a clear peak at a particular frequency and location (Figures 5B–5G). Second, some gFLs from the same recording session had similar frequencies but localized at different locations (Figures 5C, 5E, and 5G), while others displayed gamma oscillations of different frequencies at overlapping locations (Figures 5C, 5D, and 5G). Third, the spatial profiles of gFLs had elevated loading over several hundred micrometers, occasionally showing apparent localization in one cortical layer or a single cortical "column" (e.g., Figures 5C and 5E). Several location-frequency profiles of gFLs closely corresponded to those revealed by the unit-LFP spectral analysis (compare Figures 3C and 3D and Figures 5B and 5C) and local maxima analysis (Figure 4), confirming the validity of the method.

Hippocampal Theta Phase-Locking of Neocortical Gamma Oscillations

We next tested whether neocortical gamma oscillators are modulated by hippocampal theta. First, we found that the strongest theta modulation of neocortical gamma power occurred in a gamma frequency band higher than in the hippocampus (Figure 6A), eliminating volume-conduction of hippocampal gamma

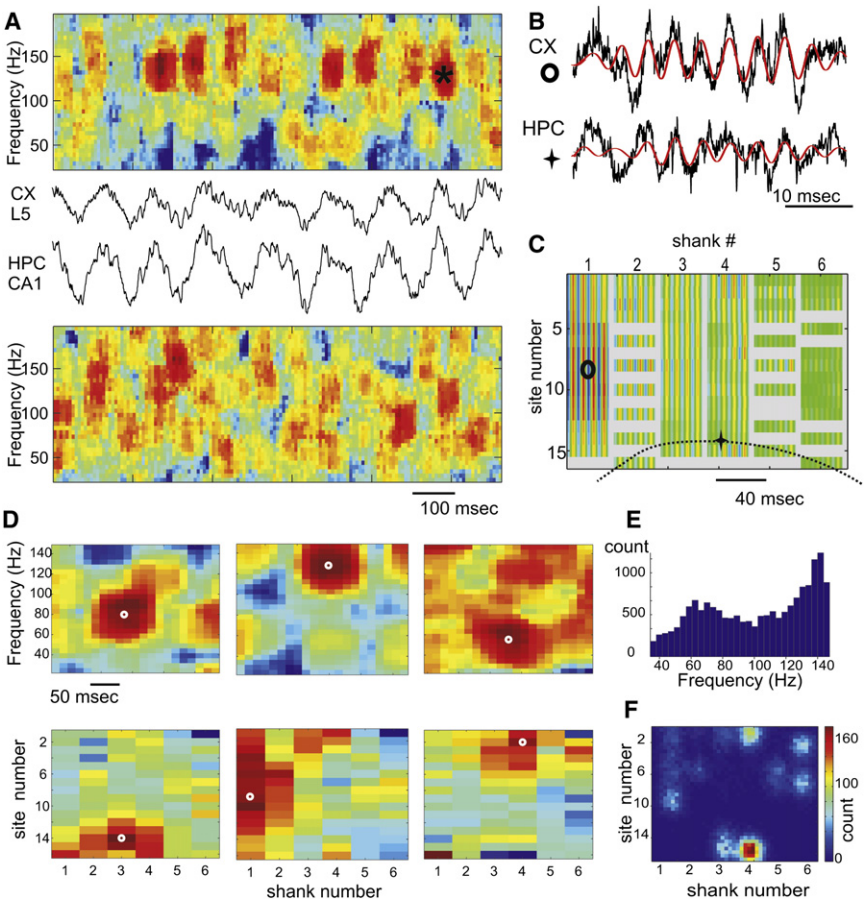

Figure 4. Temporal and Spatial Structure of Neocortical Gamma Oscillations

(A) A short epoch of neocortical (CX L5) and hippocampal (HPC CA1) LFPs and their associated "whitened" spectrograms.

(B) Gamma "burst" (red, band-pass,100–200 Hz, signal) from sites shown in (C).

(C) Color-coded spatial profile of band-pass-filtered segment in (B) at all recording sites (anatomical layout as in Figure 3A). Each column, separated by gray vertical stripes, corresponds to an electrode shank with 16 recording sites each. Malfunctioning sites are gray.

(D) Examples of isolated gamma bursts in hippocampus (left) and neocortex (middle, right). Each burst is characterized by a local maximum (white circles) of LFP spectral power (color) in both time-frequency (top) and anatomical space (bottom).

(E) Distribution of frequencies of individual local maxima. Note two modes, slow and fast gamma.

(F) Probability density of the spatial locations of local maxima of gamma power for the entire session. Note spatially segregated clusters.

to the neocortex as a potential confound. Second, in a subset of fast firing (>15 Hz) putative interneurons, we estimated the strength of unit-LFP gamma coherence at various time leads and lags from the peak of hippocampal theta (Figure 6B) and found maximum coherence on the descending slope of theta. Third, in a subset of experiments, we spatially isolated gamma bursts on the basis of power decay and clustered them in space and frequency (Figures 4D–4F). The probability of gamma bursts in some of these clusters was significantly biased by theta phase (Figure 6C). Although these separate approaches provided firm evidence for the theta phase modulation of neocortical gamma power, each of them had limitations. To overcome these limitations, we analyzed the relationship between the gFL factor score time series (which reflects the instantaneous strength of individual gamma oscillators; Figure S7) and hippocampal theta LFP (Figure 6D) and found significant coherence at theta frequency in a large fraction of the gFLs (e.g., Figure 6E). We also detected discrete times of gamma "burst" occurrence using the local maxima of the continuous gFL score time series. In a large percentage (~30%) of detected neocortical gFLs we found that gamma bursts were significantly phase modulated by hippocampal theta with the highest incidence near the peak of theta (Figures 6F–6H). High-frequency neocortical gamma bursts (>100 Hz) had stronger theta modulation and theta phase preference at a later phase (~50°; Figure 6I) than lower-frequency gamma oscillations. As expected from unit analysis, hippocampal gFL-bursts were more likely to be significantly modulated by hippocampal theta than those localized in the neocortex (60% versus 30%; Figure 6G).

Because the gFL analysis does not exploit the phase in the LFP signal, it can still be biased by the volume conduction of hippocampal gamma to the neocortex. We performed a number of analyses to rule out the contribution of the volume-conduction (see Supplemental Data). First, we estimated coherence between the gFL score and hippocampal LFP by partializing it by the hippocampal gamma power corresponding to the frequency range of the respective gFL. Approximately 90% of all gFLs (>98% for high frequency gFLs) retained a significant peak in the theta band. Second, for each gFL we computed coherence between the LFP in the center of the gFL-identified spatial gamma profile and at all other sites. The peak coherence occurred at the frequency close to the preferred frequency of the gFL (Figures S8A and S8B), with a spatial profile that matched that of the gFL (Figure 6J), providing a direct phase-synchronization measure of the local neocortical gamma. Next, we computed the integrated gamma LFP-LFP coherence within the gFL preferred frequency band in short sliding windows for the entire session and estimated the coherence between this time series and hippocampal LFP for each pair of recording sites (Figure 6K). The significant peaks at theta frequency revealed theta modulation of gamma synchronization between the LFP in the center of the gFL and spatially contiguous recording sites. If modulation of gamma power in the neocortex was a result of volume conduction of currents from the hippocampus one would expect that theta modulation of LFP-LFP coherence would increase toward hippocampus. However, in most cases the spatial profile of theta modulation of LFP-LFP gamma coherence closely matched that of the gFL and average LFP-LFP gamma

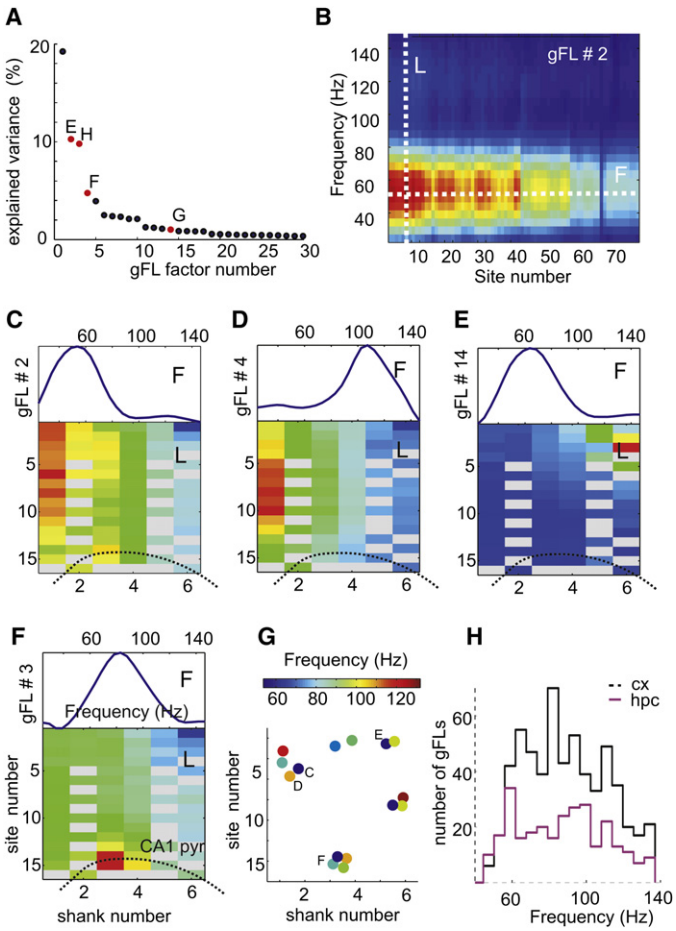

Figure 5. Spatial and Frequency Heterogeneity of Neocortical Gamma Oscillations

(A–G) Frequency-location gamma power (gFL) factor analysis (see Supplemental Data). (A) Percentage of total variance explained by the first 30 gFL factors. (B) Color-coded gFL factor loadings at 76 recording sites of the six shanks (20 malfunctioning sites removed) and gamma frequency bins (30–150 Hz). Red, positive, and blue, negative loading values. Maximal loading is localized at a given frequency (white line F) and location (white line L). (C–F) Examples of gFL factor loadings represented by frequency profile (F, top plots, loading at the maximal site across frequencies) and location profile (L, bottom, spatial maps; color indicates loading at the maximal frequency across sites) in the neocortex (C–E) and hippocampus (F). (G) Frequency (color) and spatial location of the center of mass of gFL components in a single session. Note spatial clusters of different frequency gFLs (e.g., C, D) or similar frequency preference but different locations (e.g., C, E).

(H) Distribution of the preferred frequency of cortical (n = 588, black) and hippocampal (n = 285, magenta) gFL factors.

coherence (e.g., compare Figure 5D and Figures 6J and 6K). The phase shift between gamma synchronization signal and hippocampal LFP was larger for the fast gamma, consistent with the phase preference analysis of gFL bursts (Figures S8C and S8D). Third, the spatial location of gFLs, the magnitude of theta modulation and the preferred theta phase of gFL-identified gamma bursts were similar between the first and second halves of the recording session (Figure S9), indicating that each gFL score represents the time course of an independent process. Finally, we identified a number of theta modulated gFLs in PFC, where volume-conduction of gamma is not expected due to its distance from the hippocampus. Overall, these findings indicate that hippocampal theta oscillations can exert a significant effect on local computation, represented by location and frequency-specific gamma oscillations, in wide neocortical areas.

Theta Modulation of the Membrane Potential in Neocortical Neurons

Theta phase modulation of neocortical unit discharges and gamma activity should be reflected by the membrane potential fluctuations in single neurons. To test this hypothesis, we obtained stable intracellular recordings from deep layer S1 neurons (n = 4) and biocytin-filled pyramidal cells in the mPFC (layer 2 = 1; layer 5 = 15; layer 6 = 7), together with simultaneous LFP recordings from the hippocampal CA1 pyramidal layer in an additional 27 rats anesthetized by urethane/ketamine-xylazine (Isomura et al., 2006). Hippocampal theta (3–5 Hz under anesthesia) occurred either spontaneously or was induced by tail pinching. Theta frequency oscillations of the membrane potential occurred transiently in several neocortical neurons. The intracellular voltage fluctuations occurred coherently with hippocampal theta in 16 out of 27 neurons (Figures 7A–7E). Spectral analysis of the membrane potential oscillations revealed significant power in the gamma frequency band, which fluctuated coherently with hippocampal theta (10 out of 27; Figures 7B and 7D). Both phase and strength of theta phase modulation of the membrane potential and the intracellular power of gamma were correlated with each other, although the coherence between the LFP and the membrane potential was stronger than that between the LFP and the gamma power (p = 0.004; Figures 7F and 7G). These analyses of intracellular data confirm that hippocampal theta oscillation can modulate the activity of neocortical neurons.

Volume Conduction of Hippocampal Theta Currents to the Neocortex

LFP theta oscillations in the parietal area were consistently present whenever hippocampal theta was observed, and the two theta signals co-varied in both frequency and magnitude. To examine whether LFP theta was generated by the neocortical circuits independent of hippocampal theta, we analyzed simultaneous LFP recordings in the hippocampus-neocortex axis, using multiple-site silicon probes (n = 21 sessions; Figures 8A1 and 8A2) and epidural grids (n = 9 sessions; Figures 8B1 and 8B2). In support of previous observations in anesthetized animals (Bland and Whishaw, 1976; Gerbrandt et al., 1978), the average magnitude of theta power monotonically decreased with distance from the hippocampus (Figure 8A3), and the distribution of theta power on the cortical surface reflected the physical layout of the underlying hippocampus (Figure 8B3). Theta power decreased, on average, 30%/mm in vertical direction and only 5%–10%/mm along the surface of the brain (Figure 8C). Both epidural and depth LFPs were strongly coherent with hippocampal LFP at theta frequency, with coherence

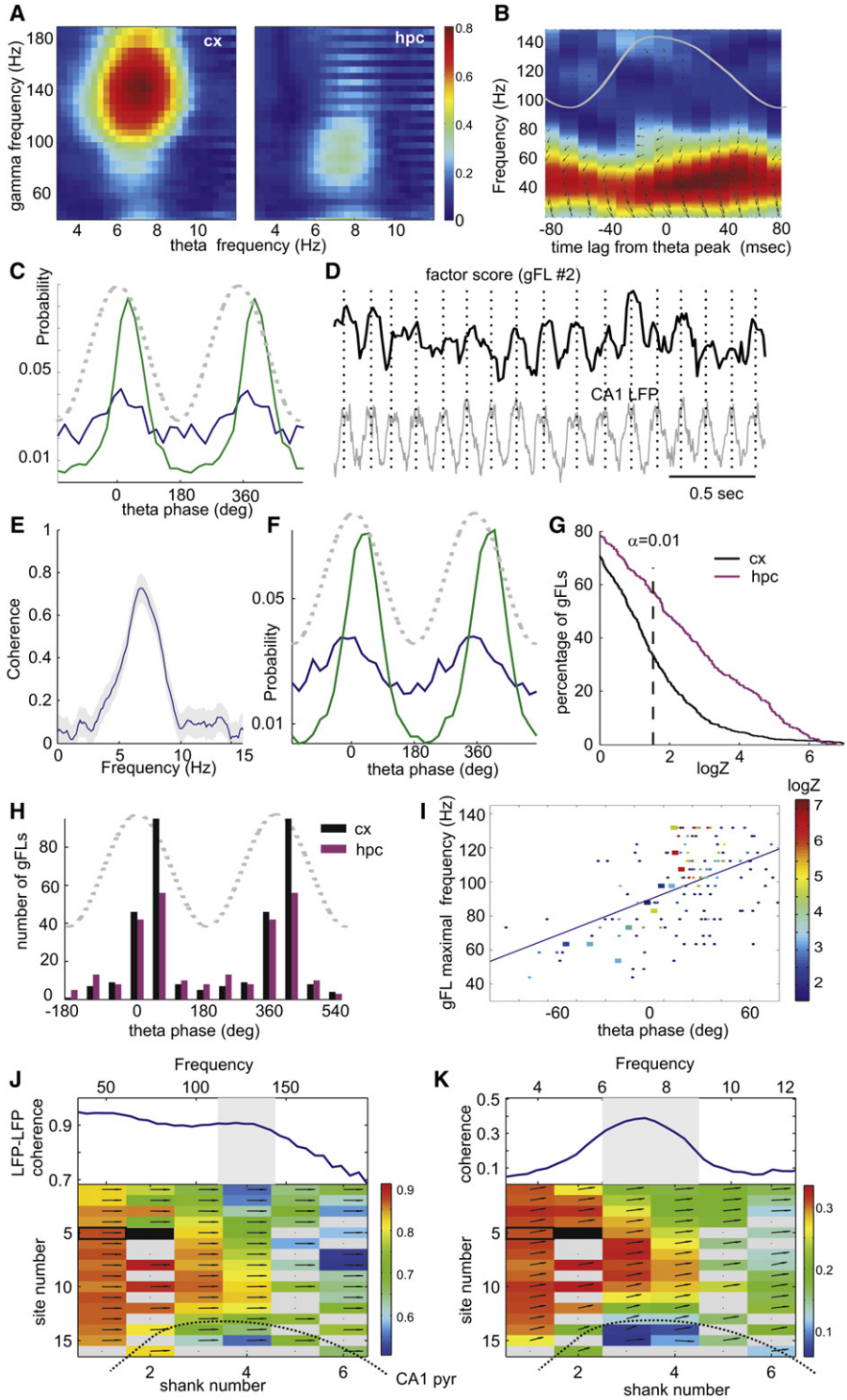

Figure 6. Hippocampal Theta Oscillations Modulate Neocortical Gamma

(A) Color-coded coherence between theta LFP in hippocampus and gamma power in different frequency bins (y axis) in the neocortex (cx) and hippocampus (hpc). Note strong modulation of higher-frequency gamma in the neocortex.

(B) Spike-LFP gamma band coherence (same unit-site pair as in Figure 3B) as a function of time lag from the peak of hippocampal theta (superimposed gray line). Small arrows, phase of spikes related to local gamma waves (zero is 3 o'clock).

(C) Theta phase histograms for two clusters of isolated gamma busts (Figures 4 E and 4F), whose spatial and frequency features correspond to those of gFL factors in Figures 5C and 5D. Dashed line, theta phase.

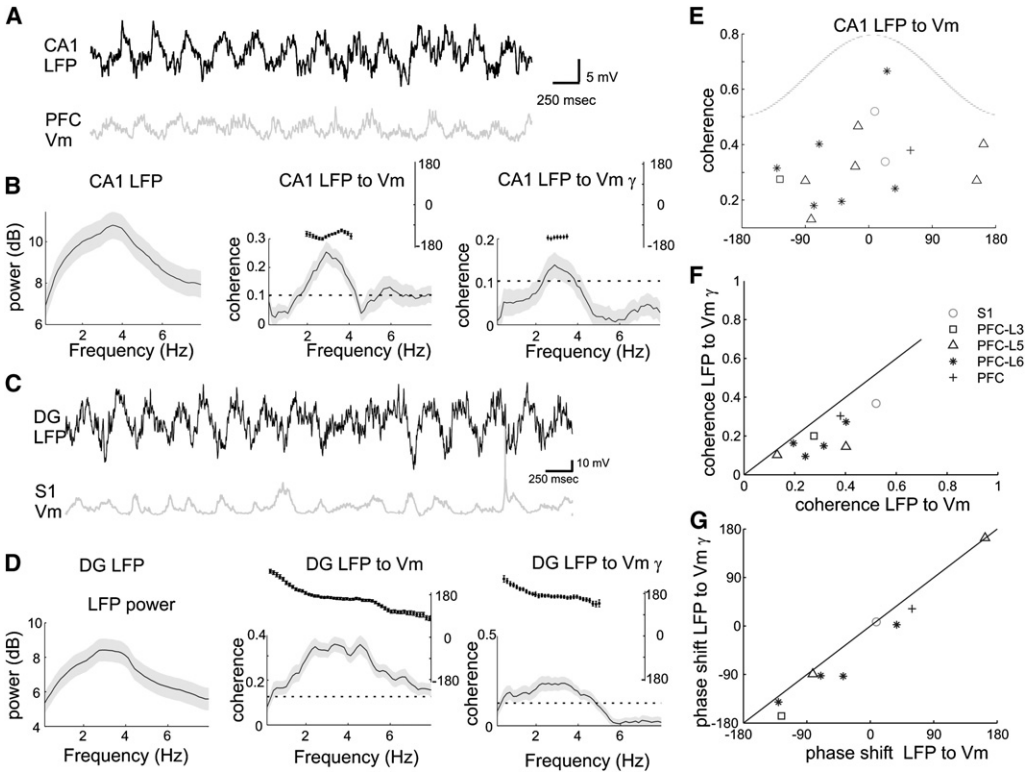

Figure 7. Theta phase Modulation of Membrane Potential in Neocortical Neurons under Anesthesia

(A) Simultaneous recording of LFP in the CA1 pyramidal layer and intracellularly recorded membrane potential in a layer 5 PFC neuron (PFC Vm).

(B) Power spectrum of the LFP (gray shading, 95 percentile confidence intervals, left); coherence between the LFP and the PFC Vm (middle); coherence between the LFP and integrated gamma power in PFC Vm (right); Inset, phase shift for the significantly coherent frequency band.

(C and D) Same display as in (A) and (B) for the simultaneous recording of LFP in the dentate gyrus (DG; theta phase ~160 degrees shifted from that in CA1) and intracellular recording from a layer 5 neuron in S1.

(E) Scatter plot of the phase shift versus the coherence value at the peak coherence frequency between CA1 LFP and Vm in cortical neurons (n = 16 significantly coherent neurons). Zero phase shift corresponds to depolarization in the Vm at the peak of hippocampal CA1 theta.

(F) Relationship between two coherence measures; coherence between the LFP and Vm versus coherence between the LFP and integrated Vm gamma power (both passed significance test).

(G) Relationship between phase shifts for cells in (F). S1, somatosensory area; PFC-L3, -L5, -L6, layers 3 to 6 of mPFC.

decaying at a rate of 5%–10%/mm (Figure 8D). Theta waves recorded between the CA1 pyramidal layer and cortical surface had approximately the same phase at all recording sites (Figure 8A4). However, the phase difference increased as a function of distance from the hippocampus in lateral and posterior directions up to 60° (e.g., Figure 8B4; n = 4 rats). Commensurate with these observations, current-source density analysis of LFP did not yield significant local sinks or sources in the theta band in the parietal area overlying the hippocampus. These findings suggest that theta measurements in the rodent neocortex are

(D) Short epoch of hippocampal theta oscillation (LFP) and factor score time series for a representative neocortical gFL (shown in Figure 5C).

(E) Coherence spectrum between the hippocampal LFP and the neocortical gFL score time series shown in (D).

(F) Theta phase histograms of neocortical "gamma bursts" (the peaks of the factor score time series) for gFLs shown in Figures 5C and 5D. Note the similarity between (C) (local maxima-based) and (F) (gFL-based) gamma burst identification.

(G) Cumulative density functions of theta phase modulation strength (logZ) for gamma bursts localized in the neocortex (black) and the hippocampus (magenta).

(H) Distribution of preferred phases of significantly ($p < 0.01$) theta-modulated gamma bursts in the neocortex (n = 280 out of 588 gFLs; black) and the hippocampus (n = 188 out of 285 gFLs; magenta).

(I) Scatterplot of the preferred theta phase of significantly modulated neocortical gamma bursts against their preferred frequency. Color indicates the strength of theta modulation statistic logZ (dots, all data; large squares, single session). Note that high-frequency gamma bursts occur at the later theta phase.

(J) Bottom, spatial map of average coherence between the LFP at the site (solid rectangle) in the center of a gFL in Figure 5D) and other sites at the gFL preferred frequency (shaded area). Top trace, example coherence for one site (open rectangle). Arrows, phase shift (zero at 3 o'clock).

(K) Top, coherence between theta LFP and gamma coherence between two neocortical sites (open rectangle and center of gFL, solid rectangle). Integrated gamma LFP-LFP coherence within the frequency band of maximum coherence (shaded range in [J]) was first computed in short sliding windows and the coherence between the resulting time series and hippocampal LFP is displayed here. Integral of this coherence in the shaded area quantifies theta modulation of gamma LFP-LFP coherence. Bottom, spatial map of theta modulation of coherence between the gFL center site (black) and other sites. See also Figure S10.

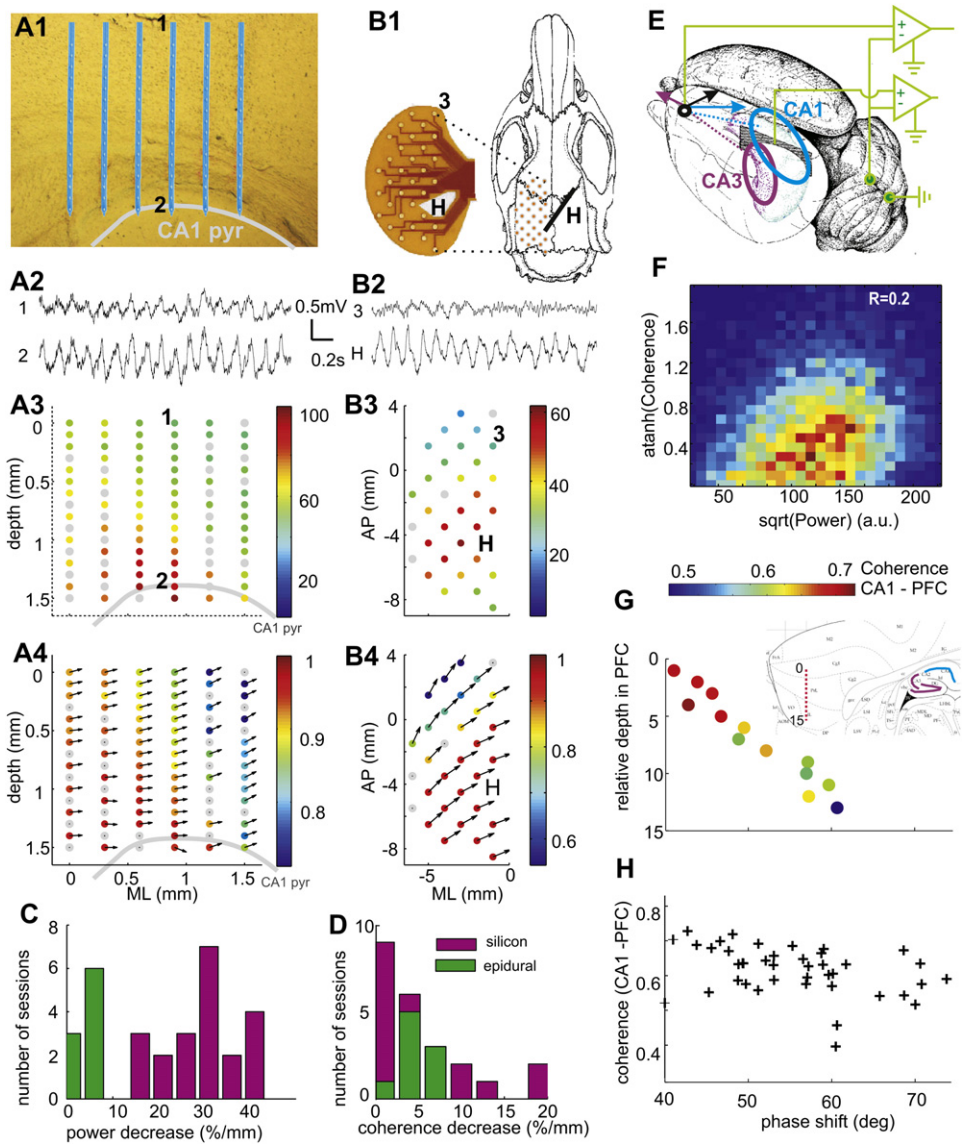

Figure 8. Volume-Conducted Hippocampal Theta Signals in the Neocortex

(A1) Position of probe shanks in the neocortex and CA1 pyramidal layer (highlighted by gray line). (A2) LFP signals from the supragranular layer of neocortex (1) and hippocampus (2). Two-dimensional map of theta power (normalized, A3) and coherence between site 2 (CA1 pyr) and other sites (A4). Theta phase shifts are indicated by arrows. Zero phase difference corresponds to 3 o'clock direction.

(B1) Layout of epidural recording of surface LFP with a flex cable (photo left). H, hippocampal depth electrode. (B2) LFP signals from site 3 of neocortex (3) and hippocampus (H). Two-dimensional map of surface theta power (B3) and coherence (B4).

(C and D) Distribution of the rate of power decrease (C) and rate coherence decrease (D) across experiments with silicon probe recordings (vertical axis, magenta) and epidural grids (horizontal axis, green).

(E) Lateral-posterior view of the left hemisphere. Arrows, hypothetical contribution of volume-conducted theta LFP vectors in PFC from the CA1 and CA3 regions (ellipsoids). The locations of ground and reference screw electrodes are also shown.

(F) Joint probability density of LFP theta power in CA1 pyr. layer and coherence between CA1 and mPFC LFP in one awake running session. Rank correlation coefficient $R = 0.2$, $p < 0.0001$.

(G) Relationship between CA1-PFC theta phase shift (coherence color-coded) and recording depth in PFC. Inset, location of the recording sites (red dots) in a sagittal section of PFC. Note monotonic phase shift and decreasing coherence with relative depth.

(H) Scatterplot of coherence between CA1 and PFC signals versus theta phase shift (n = 5 rats; REM and wake sessions combined).

dominated by the currents that are volume-conducted from the hippocampus (Bland and Whishaw, 1976; Gerbrandt et al., 1978).

LFP in the more anterior mPFC region was typically "flat" during continuous hippocampal theta oscillations (Jones and Wilson, 2005; Siapas et al., 2005) and only occasionally displayed

visible transient periods (0.5–2 s) of theta frequency oscillations (e.g., Figure 8B2). Although these intermittent theta periods were associated with increased coherence between hippocampus and PFC LFP, their occurrence was positively correlated with the power increases of hippocampal theta (Figure 8F; n = 44 sessions, rank correlation R = 0.2 ± 0.07). Moreover, LFP recorded at various depths in mPFC showed a linear phase shift and decreasing coherence referenced to the CA1 pyramidal layer (Figure 8G). Across experiments, the average CA1-mPFC coherence in the theta range was ~0.7 and the phase shift ranged from 40° to 70° (n = 25 sessions; Figure 8H). Importantly, coherence between PFC unit activity and hippocampal LFP, on average, was generally higher than the coherence between unit firing and locally recorded LFP.

Several aspects of the observations in mPFC are consistent with a volume-conductor model containing two (or more) distributed sources: e.g., CA1 and CA3/dentate regions of the hippocampus, and entorhinal cortex. Since LFP in the CA3 pyramidal layer is phase shifted (~150°) relative to CA1 pyramidal layer (cf. Buzsáki, 2002), the amplitude, phase, and coherence of theta at any location in the brain is determined by the vector summation of two (or more) volume-conducted currents (Figure 8E) and thus by the relative strength and phase of the theta generators and their relative distances from the recording site.

DISCUSSION

The major finding of the present experiments is that hippocampal theta oscillations can effectively bias the timing of local computation in the neocortex. A fraction of neurons in different neocortical areas, including the primary somatosensory area and PFC, as well as spatially localized and frequency-specific gamma oscillations were phase locked to hippocampal theta oscillations. These data suggest that theta oscillation entrainment provides a mechanism by which activity in spatially widespread neocortical and hippocampal networks can be temporally coordinated.

Hippocampal Theta Phase Locking of Neocortical Neurons

A robust finding of our experiments in both rats and mice is that 5% to 40% of neocortical neurons were significantly phase locked to hippocampal theta oscillations during either exploration or REM sleep. Importantly, theta-modulated neurons were found not only in the PFC which has massive direct afferents from the hippocampus (Swanson, 1981), but also in the primary somatosensory area, which has only multisynaptic connections with the hippocampus (Witter, 1993; Cenquizca and Swanson, 2007). The overall fraction of theta-locked units in the PFC (~35%) is comparable to that reported previously (Siapas et al., 2005), although the identity of units was not characterized in that study. These numbers should be contrasted to those in the hippocampus where, in the CA1 region, approximately 80% of the pyramidal cells and more than 90% of interneurons are significantly phase locked to theta oscillations (Figure S10; Csicsvari et al., 1999). In addition, the strength of theta modulation was considerably weaker in the neocortex, especially in the parietal cortex. These observations support the hypothesis that firing of neurons in many cortical areas is biased by the hippocampal theta oscillations (Miller, 1991).

Theta phase-locking of neocortical neurons can be brought about by multiple potential mechanisms. The simplest and oldest model assumes an independent pacemaker, residing in the septal complex (Petsche et al., 1962) and/or the supramammillary nucleus (Kocsis and Vertes, 1994), and recent studies suggest that a portion of neocortex-projecting neurons in the basal forebrain are phase-locked to hippocampal theta (Lee et al., 2005; Lin et al., 2006). An alternative mechanism of theta entrainment of distant neocortical neurons may entail the utilization of the entorhinal cortex and/or the PFC by way of their widespread, mostly reciprocal, connections with numerous neocortical regions (Groenewegen and Uylings, 2000; Swanson, 1981; Swanson and Kohler, 1986; Thierry et al., 2000; Witter, 1993). A final possibility is that hippocampo-neocortical coordination is brought about by the class of sparse long-range hippocampal projections to distant neocortical regions (Cenquizca and Swanson, 2007; Jinno et al., 2007). Any of these pathways alone or in combination may impose the hippocampal rhythmic output on their targets. The selective entrainment of a subset of neocortical neurons may be explained by either stronger synaptic connectivity between the hippocampus and selected target neocortical neurons or by the intrinsic properties of neuronal subgroups (Beierlein et al., 2000; Blatow et al., 2003; Gutfreund et al., 1995; Ulrich, 2002). Furthermore, various pharmacological manipulations can evoke theta-frequency oscillations in neocortical slices (Bao and Wu, 2003; Flint and Connors, 1996; Silva et al., 1991). Thus, theta oscillations in neocortical structures may emerge locally or/and phase-synchronize with the hippocampus via the above conduits.

The stronger entrainment of interneurons by hippocampal theta may also contribute to the enhancement of gamma oscillations (Beierlein et al., 2000; Csicsvari et al., 2003; Gibson et al., 1999; Hasenstaub et al., 2005). The similar theta phase preference of pyramidal cells and interneurons can be explained by either assuming that rhythmic afferents activated the two populations in a feed-forward manner or that local circuits are also involved in the generation of theta activity, similar to that in the CA3 hippocampal region (Buzsáki, 2002; Konopacki et al., 1987).

Locally Generated Neocortical Gamma Oscillations

Previous work has established that engagement of local circuits is reflected by the transient emergence of local gamma frequency oscillations (Bragin et al., 1995; Engel et al., 2001; Gray and Singer, 1989). We used several methods to explore neocortical gamma oscillations and demonstrated their local origin. In contrast to the hippocampus (Bragin et al., 1995; Csicsvari et al., 2003), gamma oscillations in the neocortex were transient and highly localized, confirming similar observations made with subdural grid recordings in humans (Canolty et al., 2006; Edwards et al., 2005; Howard et al., 2003; Menon et al., 1996; Sederberg et al., 2003). The amplitude of gamma oscillations decreased rapidly with distance. Gamma oscillators were often localized to either a single cortical layer and/or a putative column, consistent with previous reports (Gray and Singer, 1989; Steriade and Amzica, 1996; Sukov and Barth, 1998). Emergence of these transient fast rhythms faithfully reflects behaviorally relevant specific

computation in small networks (e.g., Gray and Singer, 1989; Montgomery and Buzsáki, 2007; Pesaran et al., 2002; Schoffelen et al., 2005; Sederberg et al., 2003). Our findings demonstrate that hippocampal theta oscillations can effectively link these sporadic and spatially distinct local gamma oscillations.

Hippocampal Theta Phase Locking of Neocortical Gamma Oscillations

Previous work has shown crossfrequency coupling between theta and gamma rhythms in the hippocampus (Bragin et al., 1995) and entorhinal cortex (Chrobak and Buzsáki, 1998a; Mormann et al., 2005). Recently, theta-gamma coupling was reported in the temporoparietal lobe of epileptic patients as well (Canolty et al., 2006). Intracranial recordings in patients also showed coupling between single unit activity and oscillations of various frequencies in the theta-gamma range (Jacobs et al., 2007). Furthermore, ''midline theta oscillations'' in human scalp recordings (Gevins et al., 1979) as well as isolated, transient neocortical theta oscillations in subdural and intracranial recordings during performance in various cognitive tasks have also been described (Caplan et al., 2003; Kahana et al., 1999; Raghavachari et al., 2001; Rizzuto et al., 2003), However, neither the mechanisms nor the origin of theta signals could be demonstrated in these clinical studies. Simultaneous recordings from the hippocampus and neocortex in our studies established that hippocampal theta oscillations exert an effect on local neocortical computation by rhythmically biasing synchrony of local gamma oscillations. We also found that neocortical fast gamma oscillations (80–150 Hz) were more strongly modulated by theta and occurred at a later phase (~50 degrees). This observation suggests that at least two distinguishable mechanisms can generate gamma oscillations in the neocortex with the higher frequency mechanism more responsive to hippocampal output (Wyart and Tallon-Baudry, 2008). The effect of theta phase-locked output on neocortical network dynamics may be analogous to that of a sensory stimulus (Engel et al., 2001; Gray and Singer, 1989; Sukov and Barth, 1998) since both effects can induce localized gamma oscillations. The widespread synchronization of neocortical neuronal assemblies by the hippocampal theta rhythm might provide a mechanism for ''gating'' of sensory information and temporally biasing movement initiation by the hippocampal theta rhythm (Bland, 1986).

Volume Conduction of Hippocampal Theta to the Neocortex

Using a combination of approaches, including epidural grid and silicon probe recordings of LFP, our findings support previous suggestions that theta signals in a large expanse of the rat neocortex and other proximal structures are largely volume conducted from the hippocampus and/or entorhinal cortex (Bland and Whishaw, 1976; Gerbrandt et al., 1978). Coherence of theta signals was attenuated monotonically as a function of both vertical and horizontal distance from the hippocampus, with a predictable phase shift between hippocampal and neocortical recording sites. If theta signal represented a single periodic dipole and originated from a point source, its attenuation and phase could be calculated from the biophysical features of the conducting brain tissue (Logothetis et al., 2007). However, theta is a consortium of several oscillators generated by multiple hippocampal-entorhinal regions and mechanisms, and both the power and phase relation of the generators vary as a function of behavior (Buzsáki, 2002). The important consequence of this complex relationship is that LFP signals recorded from cortical or subcortical sites in the rodent may reflect superposition of volume-conducted currents from two or more spatially distributed current sources in the hippocampus (Figure 8E) and the entorhinal cortex. The implication of the multiple-source volume-conductor model is that the amplitude, phase, and degree of coherence to hippocampal theta of extrahippocampally recorded theta signals may show systematic variations with behavior, yet such changes may arise entirely from intrahippocampal mechanisms.

These observations and considerations, of course, do not exclude neocortical generation of theta oscillations (Caplan et al., 2003; Ishii et al., 1999; Kahana et al., 1999; Raghavachari et al., 2001; Rizzuto et al., 2003). Importantly, we found that a small portion of PFC theta bursts was different in frequency from hippocampal theta (not shown), indicating that PFC circuits can generate LFP in the theta frequency band (Siapas et al., 2005; Jones and Wilson, 2005). However, when such transient epochs are of the *same* frequency as hippocampal theta, disambiguating locally generated currents and volume-conducted currents becomes difficult with currently available LFP recording methods.

Reciprocal Information Transfer by Theta Oscillations

Transfer of information in the brain from source (sender) to target (receiver) is usually considered unidirectional: the source network sends the information to a recipient network (Abeles, 1991). Oscillatory entrainment, however, allows for a different mechanism of information exchange, which we refer to as ''reciprocal information transfer.'' In this hypothetical mechanism, we assume that the recipient structure plays an initiating role by temporally biasing activity in the source structure, creating time windows within which the recipient structure can most effectively receive information (Fries, 2005; Isomura et al., 2006; Sirota et al., 2003; Sirota and Buzsáki, 2007; Womelsdorf et al., 2007). For example, experiments suggest that during slow wave sleep transfer of hippocampal information to the neocortex is initiated by the down-up transition of neocortical slow oscillation (Isomura et al., 2006; Sirota et al., 2003; Sirota and Buzsáki, 2007). In a similar manner, we suggest that transfer of neocortical information to the hippocampus is actively initiated by the hippocampus via theta-phase biasing of neocortical network dynamics. As a result, self-organized gamma oscillations at multiple cortical locations is temporally biased so that the information contained in the gamma bursts would arrive at the hippocampus at the phase of the theta cycle when the network can be perturbed maximally and when it is most plastic (Holscher et al., 1997; Huerta and Lisman, 1996; Hyman et al., 2003), which, in the case of CA1 pyramidal cells, corresponds to the positive (least active) phase of the theta cycle (Csicsvari et al., 1999). In this context, it is noteworthy that hippocampal neurons begin to discharge at this late (positive) phase when the rat enters the place field of the neuron (O'Keefe and Recce, 1993), likely triggered by the cooperative action of neocortical assemblies.

The postulated model of reciprocal information transfer can ensure that information from wide areas of the neocortex can be presented to the hippocampus in a temporally synchronous manner and integrated into its associative networks.

EXPERIMENTAL PROCEDURES

Animals and Recording

Chronic recordings in the neocortex and hippocampus using silicon probes, tetrodes, or epidural electrodes were performed in rats (n = 28) and mice (n = 11) during sleep and waking behavior. Acute extracellular recordings in the hippocampus and intracellular recordings in the neocortex were performed in anesthetized rats (n = 27; Isomura et al., 2006).

Data Analysis

All analysis was performed using custom-written tools in Matlab (Mathworks). For detailed description, see Supplemental Data.

SUPPLEMENTAL DATA

The Supplemental Data include Ten Figures and Supplemental Experimental Procedures and can be found with this article online at http://www.neuron.org/supplemental/S0896-6273(08)00762-9.

ACKNOWLEDGMENTS

We thank Asohan Amarasigham, Carina Curto, Kamran Diba, Caroline Geisler, Kenji Mizuseki, Simal Ozen, Lucas Parra, and Alfonso Renart for useful discussions and comments on the manuscript; Derek Buhl and Dirk Isbrandt for providing recordings in mice; Alexei Ponomarenko and Matthew Guilfoyle for assisting with recordings; Darrell A. Henze for intracellular recordings from somatosensory cortex; and John Bentley and Michael Stephens for help with statistical analysis of the mixture model. Supported by National Institutes of Health (NS034994; MH54671), National Science Foundation (SBE0542013), the J.D. McDonnell Foundation, Uehara Memorial Foundation, and the Japan Society of Promotion for Sciences.

Accepted: September 4, 2008
Published: November 25, 2008

REFERENCES

Abeles, M. (1991). Corticonics: Neural Circuits of the Cerebral Cortex (Cambridge: Cambridge University Press).

Alonso, A., and Garcia-Austt, E. (1987). Neuronal sources of theta rhythm in the entorhinal cortex of the rat. II. Phase relations between unit discharges and theta field potentials. Exp. Brain Res. *67*, 502–509.

Anderson, M.I., and O'Mara, S.M. (2003). Analysis of recordings of single-unit firing and population activity in the dorsal subiculum of unrestrained freely moving rats. J. Neurophysiol. *90*, 655–665.

Bao, W., and Wu, J.Y. (2003). Propagating wave and irregular dynamics: spatiotemporal patterns of cholinergic theta oscillations in neocortex in vitro. J. Neurophysiol. *90*, 333–341.

Barthó, P., Hirase, H., Monconduit, L., Zugaro, M., Harris, K.D., and Buzsáki, G. (2004). Characterization of neocortical principal cells and interneurons by network interactions and extracellular features. J. Neurophysiol. *92*, 600–608.

Beierlein, M., Gibson, J.R., and Connors, B.W. (2000). A network of electrically coupled interneurons drives synchronized inhibition in neocortex. Nat. Neurosci. *3*, 904–910.

Berg, R.W., Whitmer, D., and Kleinfeld, D. (2006). Exploratory whisking by rat is not phase locked to the hippocampal theta rhythm. J. Neurosci. *26*, 6518–6522.

Bland, B.H. (1986). The physiology and pharmacology of hippocampal formation theta rhythms. Prog. Neurobiol. *26*, 1–54.

Bland, B.H., and Whishaw, I.Q. (1976). Generators and topography of hippocampal theta (RSA) in the anaesthetized and freely moving rat. Brain Res. *118*, 259–280.

Blatow, M., Rozov, A., Katona, I., Hormuzdi, S.G., Meyer, A.H., Whittington, M.A., Caputi, A., and Monyer, H. (2003). A novel network of multipolar bursting interneurons generates theta frequency oscillations in neocortex. Neuron *38*, 805–817.

Bragin, A., Jando, G., Nadasdy, Z., Hetke, J., Wise, K., and Buzsáki, G. (1995). Gamma (40–100 Hz) oscillation in the hippocampus of the behaving rat. J. Neurosci. *15*, 47–60.

Buño, W., Jr., and Velluti, J.C. (1977). Relationships of hippocampal theta cycles with bar pressing during self-stimulation. Physiol. Behav. *19*, 615–621.

Buzsáki, G. (2002). Theta oscillations in the hippocampus. Neuron *33*, 325–340.

Buzsáki, G. (2006). Rhythms of the Brain (New York: Oxford University Press).

Canolty, R.T., Edwards, E., Dalal, S.S., Soltani, M., Nagarajan, S.S., Kirsch, H.E., Berger, M.S., Barbaro, N.M., and Knight, R.T. (2006). High gamma power is phase-locked to theta oscillations in human neocortex. Science *313*, 1626–1628.

Caplan, J.B., Madsen, J.R., Schulze-Bonhage, A., Aschenbrenner-Scheibe, R., Newman, E.L., and Kahana, M.J. (2003). Human theta oscillations related to sensorimotor integration and spatial learning. J. Neurosci. *23*, 4726–4736.

Cenquizca, L.A., and Swanson, L.W. (2007). Spatial organization of direct hippocampal field CA1 axonal projections to the rest of the cerebral cortex. Brain Res. Brain Res. Rev. *56*, 1–26.

Chrobak, J.J., and Buzsáki, G. (1998a). Gamma oscillations in the entorhinal cortex of the freely behaving rat. J. Neurosci. *18*, 388–398.

Chrobak, J.J., and Buzsáki, G. (1998b). Operational dynamics in the hippocampal-entorhinal axis. Neurosci. Biobehav. Rev. *22*, 303–310.

Collins, D.R., Lang, E.J., and Paré, D. (1999). Spontaneous activity of the perirhinal cortex in behaving cats. Neuroscience *89*, 1025–1039.

Colom, L.V., Christie, B.R., and Bland, B.H. (1988). Cingulate cell discharge patterns related to hippocampal EEG and their modulation by muscarinic and nicotinic agents. Brain Res. *460*, 329–338.

Constantinidis, C., and Goldman-Rakic, P.S. (2002). Correlated discharges among putative pyramidal neurons and interneurons in the primate prefrontal cortex. J. Neurophysiol. *88*, 3487–3497.

Csicsvari, J., Hirase, H., Czurko, A., Mamiya, A., and Buzsáki, G. (1999). Oscillatory coupling of hippocampal pyramidal cells and interneurons in the behaving rat. J. Neurosci. *19*, 274–287.

Csicsvari, J., Jamieson, B., Wise, K.D., and Buzsáki, G. (2003). Mechanisms of gamma oscillations in the hippocampus of the behaving rat. Neuron *37*, 311–322.

Dehaene, S., Sergent, C., and Changeux, J.P. (2003). A neuronal network model linking subjective reports and objective physiological data during conscious perception. Proc. Natl. Acad. Sci. USA *100*, 8520–8525.

Destexhe, A., and Sejnowski, T. (2001). Thalamocortical Assemblies—How Ion Channels, Single Neurons and Large-Scale Networks Organize Sleep Oscillations (Oxford: Oxford University Press).

Edwards, E., Soltani, M., Deouell, L.Y., Berger, M.S., and Knight, R.T. (2005). High gamma activity in response to deviant auditory stimuli recorded directly from human cortex. J. Neurophysiol. *94*, 4269–4280.

Engel, A.K., Fries, P., and Singer, W. (2001). Dynamic predictions: oscillations and synchrony in top-down processing. Nat. Rev. Neurosci. *2*, 704–716.

Flint, A.C., and Connors, B.W. (1996). Two types of network oscillations in neocortex mediated by distinct glutamate receptor subtypes and neuronal populations. J. Neurophysiol. *75*, 951–957.

Freund, T.F., and Buzsáki, G. (1996). Interneurons of the hippocampus. Hippocampus *6*, 347–470.

Fries, P. (2005). A mechanism for cognitive dynamics. Neuronal communication through neuronal coherence. Trends Cogn Sci. *9*, 474–480.

Gerbrandt, L.K., Lawrence, J.C., Eckardt, M.J., and Lloyd, R.L. (1978). Origin of the neocortically monitored theta rhythm in the curarized rat. Electroencephalogr. Clin. Neurophysiol. *45*, 454–467.

Gevins, A.S., Zeitlin, G.M., Doyle, J.C., Yingling, C.D., Schaffer, R.E., Callaway, E., and Yeager, C.L. (1979). Electroencephalogram correlates of higher cortical functions. Science *203*, 665–668.

Gibson, J.R., Beierlein, M., and Connors, B.W. (1999). Two networks of electrically coupled inhibitory neurons in neocortex. Nature *402*, 75–79.

Grastyán, E., Lissák, K., Madarász, I., and Donhoffer, H. (1959). The hippocampal electrical activity during the development of conditioned reflexes. Electroencephalogr. Clin. Neurophysiol. *11*, 409–430.

Gray, C.M., and Singer, W. (1989). Stimulus-specific neuronal oscillations in orientation columns of cat visual cortex. Proc. Natl. Acad. Sci. USA *86*, 1698–1702.

Green, J.D., and Arduni, A.A. (1954). Hippocampal electrical activity in arousal. J. Neurophysiol. *17*, 533–557.

Groenewegen, H.J., and Uylings, H.B. (2000). The prefrontal cortex and the integration of sensory, limbic and autonomic information. Prog. Brain Res. *126*, 3–28.

Gutfreund, Y., Yarom, Y., and Segev, I. (1995). Subthreshold oscillations and resonant frequency in guinea-pig cortical neurons: physiology and modelling. J. Physiol. *483*, 621–640.

Harris, K.D., Csicsvari, J., Hirase, H., Dragoi, G., and Buzsáki, G. (2003). Organization of cell assemblies in the hippocampus. Nature *424*, 552–556.

Hasenstaub, A., Shu, Y., Haider, B., Kraushaar, U., Duque, A., and Mccormick, D.A. (2005). Inhibitory postsynaptic potentials carry synchronized frequency information in active cortical networks. Neuron *47*, 423–435.

Holscher, C., Anwyl, R., and Rowan, M.J. (1997). Stimulation on the positive phase of hippocampal theta rhythm induces long-term potentiation that can be depotentiated by stimulation on the negative phase in area CA1 in vivo. J. Neurosci. *17*, 6470–6477.

Holsheimer, J. (1982). Generation of theta activity (RSA) in the cingulate cortex of the rat. Exp. Brain Res. *47*, 309–312.

Howard, M.W., Rizzuto, D.S., Caplan, J.B., Madsen, J.R., Lisman, J., Aschenbrenner-Scheibe, R., Schulze-Bonhage, A., and Kahana, M.J. (2003). Gamma oscillations correlate with working memory load in humans. Cereb. Cortex *13*, 1369–1374.

Huerta, P.T., and Lisman, J.E. (1996). Low-frequency stimulation at the troughs of theta-oscillation induces long-term depression of previously potentiated CA1 synapses. J. Neurophysiol. *75*, 877–884.

Hyman, J.M., Wyble, B.P., Goyal, V., Rossi, C.A., and Hasselmo, M.E. (2003). Stimulation in hippocampal region CA1 in behaving rats yields long-term potentiation when delivered to the peak of theta and long-term depression when delivered to the trough. J. Neurosci. *23*, 11725–11731.

Hyman, J.M., Zilli, E.A., Paley, A.M., and Hasselmo, M.E. (2005). Medial prefrontal cortex cells show dynamic modulation with the hippocampal theta rhythm dependent on behavior. Hippocampus *15*, 739–749.

Ishii, R., Shinosaki, K., Ukai, S., Inouye, T., Ishihara, T., Yoshimine, T., Hirabuki, N., Asada, H., Kihara, T., Robinson, S.E., and Takeda, M. (1999). Medial prefrontal cortex generates frontal midline theta rhythm. Neuroreport *10*, 675–679.

Isomura, Y., Sirota, A., Ozen, S., Montgomery, S., Mizuseki, K., Henze, D.A., and Buzsáki, G. (2006). Integration and segregation of activity in entorhinal-hippocampal subregions by neocortical slow oscillations. Neuron *52*, 871–882.

Jacobs, J., Kahana, M.J., Ekstrom, A.D., and Fried, I. (2007). Brain oscillations control timing of single-neuron activity in humans. J. Neurosci. *27*, 3839–3844.

Jinno, S., Klausberger, T., Marton, L.F., Dalezios, Y., Roberts, J.D., Fuentealba, P., Bushong, E.A., Henze, D., Buzsáki, G., and Somogyi, P. (2007). Neuronal diversity in gabaergic long-range projections from the hippocampus. J. Neurosci. *27*, 8790–8804.

Jones, M.W., and Wilson, M.A. (2005). Theta rhythms coordinate hippocampal-prefrontal interactions in a spatial memory task. PLoS Biol. *3*, e402. 10.1371/journal.pbio.0030402.

Jouvet, M. (1969). Biogenic amines and the states of sleep. Science *163*, 32–41.

Kahana, M.J., Sekuler, R., Caplan, J.B., Kirschen, M., and Madsen, J.R. (1999). Human theta oscillations exhibit task dependence during virtual maze navigation. Nature *399*, 781–784.

Kocsis, B., and Vertes, R.P. (1994). Characterization of neurons of the supramammillary nucleus and mammillary body that discharge rhythmically with the hippocampal theta rhythm in the rat. J. Neurosci. *14*, 7040–7052.

Konopacki, J., Bland, B.H., Maciver, M.B., and Roth, S.H. (1987). Cholinergic theta rhythm in transected hippocampal slices: independent CA1 and dentate generators. Brain Res. *436*, 217–222.

Lakatos, P., Shah, A.S., Knuth, K.H., Ulbert, I., Karmos, G., and Schroeder, C.E. (2005). An oscillatory hierarchy controlling neuronal excitability and stimulus processing in the auditory cortex. J. Neurophysiol. *94*, 1904–1911.

Lee, M.G., Hassani, O.K., Alonso, A., and Jones, B.E. (2005). Cholinergic basal forebrain neurons burst with theta during waking and paradoxical sleep. J. Neurosci. *25*, 4365–4369.

Leung, L.W., and Borst, J.G. (1987). Electrical activity of the cingulate cortex. I. Generating mechanisms and relations to behavior. Brain Res. *407*, 68–80.

Lin, S.C., Gervasoni, D., and Nicolelis, M.A. (2006). Fast modulation of prefrontal cortex activity by basal forebrain noncholinergic neuronal ensembles. J. Neurophysiol. *96*, 3209–3219.

Logothetis, N.K., Kayser, C., and Oeltermann, A. (2007). In vivo measurement of cortical impedance spectrum in monkeys: implications for signal propagation. Neuron *55*, 809–823.

Macrides, F., Eichenbaum, H.B., and Forbes, W.B. (1982). Temporal relationship between sniffing and the limbic theta rhythm during odor discrimination reversal learning. J. Neurosci. *2*, 1705–1717.

Markram, H. (2006). The blue brain project. Nat. Rev. Neurosci. *7*, 153–160.

Menon, V., Freeman, W.J., Cutillo, B.A., Desmond, J.E., Ward, M.F., Bressler, S.L., Laxer, K.D., Barbaro, N., and Gevins, A.S. (1996). Spatio-temporal correlations in human gamma band electrocorticograms. Electroencephalogr. Clin. Neurophysiol. *98*, 89–102.

Miller, R. (1991). Cortico-Hippocampal Interplay (New York: Springer-Verlag).

Montgomery, S.M., and Buzsáki, G. (2007). Gamma oscillations dynamically couple hippocampal CA3 and CA1 regions during memory task performance. Proc. Natl. Acad. Sci. USA *104*, 14495–14500.

Mormann, F., Fell, J., Axmacher, N., Weber, B., Lehnertz, K., Elger, C.E., and Fernandez, G. (2005). Phase/amplitude reset and theta-gamma interaction in the human medial temporal lobe during a continuous word recognition memory task. Hippocampus *15*, 890–900.

Muir, G.M., and Bilkey, D.K. (1998). Synchronous modulation of perirhinal cortex neuronal activity during cholinergically mediated (type II) hippocampal theta. Hippocampus *8*, 526–532.

O'Keefe, J., and Burgess, N. (2005). Dual phase and rate coding in hippocampal place cells: theoretical significance and relationship to entorhinal grid cells. Hippocampus *15*, 853–866.

O'Keefe, J., and Recce, M.L. (1993). Phase relationship between hippocampal place units and the EEG theta rhythm. Hippocampus *3*, 317–330.

Paré, D., and Gaudreau, H. (1996). Projection cells and interneurons of the lateral and basolateral amygdala. Distinct firing patterns and differential relation to theta and delta rhythms in conscious cats. J. Neurosci. *16*, 3334–3350.

Pesaran, B., Pezaris, J.S., Sahani, M., Mitra, P.P., and Andersen, R.A. (2002). Temporal structure in neuronal activity during working memory in macaque parietal cortex. Nat. Neurosci. *5*, 805–811.

Petsche, H., Stumpf, C., and Gogolak, G. (1962). The significance of the rabbit's septum as a relay station between the midbrain and the hippocampus. I. The control of hippocampus arousal activity by the septum cells. Electroencephalogr. Clin. Neurophysiol. *14*, 202–211.

Raghavachari, S., Kahana, M.J., Rizzuto, D.S., Caplan, J.B., Kirschen, M.P., Bourgeois, B., Madsen, J.R., and Lisman, J.E. (2001). Gating of human theta oscillations by a working memory task. J. Neurosci. *21*, 3175–3183.

Rizzuto, D.S., Madsen, J.R., Bromfield, E.B., Schulze-Bonhage, A., Seelig, D., Aschenbrenner-Scheibe, R., and Kahana, M.J. (2003). Reset of human neocortical oscillations during a working memory task. Proc. Natl. Acad. Sci. USA *100*, 7931–7936.

Schoffelen, J.M., Oostenveld, R., and Fries, P. (2005). Neuronal coherence as a mechanism of effective corticospinal interaction. Science *308*, 111–113.

Sederberg, P.B., Kahana, M.J., Howard, M.W., Donner, E.J., and Madsen, J.R. (2003). Theta and gamma oscillations during encoding predict subsequent recall. J. Neurosci. *23*, 10809–10814.

Semba, K., and Komisaruk, B.R. (1978). Phase of the theta wave in relation to different limb movements in awake rats. Electroencephalogr. Clin. Neurophysiol. *44*, 61–71.

Siapas, A.G., Lubenov, E.V., and Wilson, M.A. (2005). Prefrontal phase locking to hippocampal theta oscillations. Neuron *46*, 141–151.

Silva, L.R., Amitai, Y., and Connors, B.W. (1991). Intrinsic oscillations of neocortex generated by layer 5 pyramidal neurons. Science *251*, 432–435.

Sirota, A., and Buzsáki, G. (2007). Interaction between neocortical and hippocampal networks via slow oscillations. Thalamus Relat. Syst. *3*, 245–259.

Sirota, A., Csicsvari, J., Buhl, D., and Buzsáki, G. (2003). Communication between neocortex and hippocampus during sleep in rodents. Proc. Natl. Acad. Sci. USA *100*, 2065–2069.

Somogyi, P., and Klausberger, T. (2005). Defined types of cortical interneurone structure space and spike timing in the hippocampus. J. Physiol. *562*, 9–26.

Steriade, M., and Amzica, F. (1996). Intracortical and corticothalamic coherency of fast spontaneous oscillations. Proc. Natl. Acad. Sci. USA *93*, 2533–2538.

Sukov, W., and Barth, D.S. (1998). Three-dimensional analysis of spontaneous and thalamically evoked gamma oscillations in auditory cortex. J. Neurophysiol. *79*, 2875–2884.

Swanson, L.W. (1981). A direct projection from ammon's horn to prefrontal cortex in the rat. Brain Res. *217*, 150–154.

Swanson, L.W., and Kohler, C. (1986). Anatomical evidence for direct projections from the entorhinal area to the entire cortical mantle in the rat. J. Neurosci. *6*, 3010–3023.

Thierry, A.M., Gioanni, Y., Degenetais, E., and Glowinski, J. (2000). Hippocampo-prefrontal cortex pathway: anatomical and electrophysiological characteristics. Hippocampus *10*, 411–419.

Tierney, P.L., Degenetais, E., Thierry, A.M., Glowinski, J., and Gioanni, Y. (2004). Influence of the hippocampus on interneurons of the rat prefrontal cortex. Eur. J. Neurosci. *20*, 514–524.

Ulrich, D. (2002). Dendritic resonance in rat neocortical pyramidal cells. J. Neurophysiol. *87*, 2753–2759.

Vanderwolf, C.H. (1969). Hippocampal electrical activity and voluntary movement in the rat. Electroencephalogr. Clin. Neurophysiol. *26*, 407–418.

Varela, F., Lachaux, J.P., Rodriguez, E., and Martinerie, J. (2001). The brainweb: phase synchronization and large-scale integration. Nat. Rev. Neurosci. *2*, 229–239.

Vertes, R.P., Albo, Z., and Viana, D.P. (2001). Theta-rhythmically firing neurons in the anterior thalamus: implications for mnemonic functions of Papez's circuit. Neuroscience *104*, 619–625.

Witter, M.P. (1993). Organization of the entorhinal-hippocampal system: a review of current anatomical data. Hippocampus *3 Spec No*, 33–44.

Womelsdorf, T., Schoffelen, J.M., Oostenveld, R., Singer, W., Desimone, R., Engel, A.K., and Fries, P. (2007). Modulation of neuronal interactions through neuronal synchronization. Science *316*, 1609–1612.

Wyart, V., and Tallon-Baudry, C. (2008). Neural dissociation between visual awareness and spatial attention. J. Neurosci. *28*, 2667–2679.